Current Biology, Vol. 14, 184–196, February 3, 2004, ©2004 Elsevier Science Ltd. All rights reserved. DOI 10.1016/j.cub.2004.01.026

The Anterior-Posterior Axis Emerges Respecting the Morphology of the Mouse Embryo that Changes and Aligns with the Uterus before Gastrulation

Daniel Mesnard,[1,4] Mario Filipe,[2,4] José A. Belo,[2,3,5] and Magdalena Zernicka-Goetz[1,*]
[1]Wellcome Trust/Cancer Research Gurdon Institute
Tennis Court Road
Cambridge CB2 1QR
United Kingdom
[2]Instituto Gulbenkian de Ciencia
Rua da Quinta Grande, 6. Apartado 14
2781-901 Oeiras
Portugal
[3]Faculdade de Engenharia de Recursos Naturais
Universidade do Algarve, Campus de Gambelas
8000-010 Faro
Portugal

Summary

Background: When the anterior-posterior axis of the mouse embryo becomes explicit at gastrulation, it is almost perpendicular to the long uterine axis. This led to the belief that the uterus could play a key role in positioning this future body axis.
Results: Here, we demonstrate that when the anterior-posterior axis first emerges it does not respect the axes of the uterus but, rather, the morphology of the embryo. Unexpectedly, the emerging anterior-posterior axis is initially aligned not with the long, but the short axis of the embryo. Then whether the embryo develops in vitro or in utero, the anterior-posterior axis becomes aligned with the long axis of embryo just prior to gastrulation. Of three mechanisms that could account for this apparent shift in anterior-posterior axis orientation–cell migration, spatial change of gene expression, or change in embryo shape–lineage tracing studies favor a shape change accompanied by restriction of the expression domain of anterior markers. This property of the embryo must be modulated by interactions with the uterus as ultimately the anterior-posterior and long axes of the embryo align with the left-right uterine axis.
Conclusions: The emerging anterior-posterior axis relates to embryo morphology rather than that of the uterus. The apparent shift in its orientation to align with the long embryonic axis and with the uterus is associated with a change in embryo shape and a refinement of anterior gene expression pattern. This suggests an interdependence between anterior-posterior gene expression, the shape of the embryo, and the uterus.

Introduction

The anterior-posterior axis of the mouse embryo becomes morphologically explicit at embryonic day (E) 6.5. However, the first molecular signs of the anterior-posterior polarity after implantation appear at E5.5 and are revealed by the asymmetric expression of several genes along the proximal-distal axis of the egg cylinder [1]. Thus, while the mouse embryo appears radially symmetrical at E5.5, embryonic patterning is evident along the proximal-distal axis, with extraembryonic ectoderm located proximally, epiblast distally, and visceral endoderm enveloping both tissues. Within these tissues, gene expression patterns further define subdomains of asymmetry along the proximal-distal axis. *Bmp4*, for example, becomes progressively restricted to the distal part of the extraembryonic ectoderm [2], nodal and *Wnt3* to the adjacent proximal epiblast [3–5], and *Hex* or *Cerberus-like* are specifically expressed in a discrete set of visceral endoderm cells at the distal tip of the egg cylinder [7–10]. Thus, the emergence of molecular pathways determining axial organization of the postimplantation embryo can be detected along the proximal-distal axis at this stage.

A second "step" involved in determining axial organization of the postimplantation embryo relates to cell movement. At E5.5, distal visceral endoderm cells initiate asymmetric migration toward the site that will become the anterior [6, 11–12]. As this movement occurs, genes (such as *Fgf8* or *Wnt3*) known to be expressed radially in the proximal epiblast become restricted in their expression toward the future posterior side of the egg cylinder defined by the site of primitive streak formation [1]. Since migrating anterior visceral endoderm (AVE) cells produce Nodal and Wnt antagonists, it is believed that the AVE imparts anterior identity on the underlying epiblast by protecting it from signals that promote the formation of the primitive streak at the posterior [12–14]. Asymmetric cell movements thus permit anterior-posterior asymmetry to be established and to emerge correctly orientated [15]. Whether the orientation of this asymmetric cell migration and consequently of the anterior-posterior axis is random or occurs as a response to a symmetry breaking cue has remained unknown.

There are two common suspects for such a cue: one prediction is that it relates to the site of embryo implantation, another is that it relates to the intrinsic polarity of the embryo itself. These possibilities do not have to be mutually exclusive. Orientation of the embryo as it implants into the uterus relates to polarity developed by the blastocyst stage [16–19]. Perhaps, therefore, the embryo could respond asymmetrically to putative signals coming from this new maternal environment. Thus, regardless of whether or not the orientation of the implanting embryo itself is predetermined by its intrinsic asymmetry, it is possible that the uterus influences the development of anterior-posterior polarity. The second possibility is that this polarity stems from intrinsic asymmetry in the embryo itself; this could develop (at least initially) independently of the uterus. This finds some support from the discovery that certain aspects of the proximal-distal polarity of the egg cylinder can be traced back to the axis of bilateral symmetry of the preimplanta-

*Correspondence: mzg@mole.bio.cam.ac.uk
[4]These authors contributed equally to this work.
[5]Animal requests should be addressed to José A. Belo (jbelo@igc.gulbenkian.pt).

tion blastocyst, which in turn relates to the animal-vegetal axis of the zygote [11, 19–21]. The visceral endoderm progeny of cells from the end of the blastocyst axis derived from the animal pole tend to become positioned more distally on the egg cylinder than those derived from the vegetal pole [11].

Another intriguing observation that emerged from the studies of Weber and colleagues [11] was the changing shape of the clones of visceral endoderm cells as development proceeds from blastocyst to the egg cylinder stages. The coherent clones in the extraembryonic part were often diagonal extending from the anterior-proximal to posterior-distal regions, reflecting asymmetric cell behavior. Clones in the embryonic part tended to be dispersed, consistent with posterior-to-anterior movement in the midline and spiraling in the lateral regions [11]. This indicated that even though the nature and extent of cell displacements in these two parts of the egg cylinder differ, the visceral endoderm behavior in both extraembryonic and embryonic parts reflected the emerging anterior-posterior polarity. These studies thus provided us with a glimpse of a complex pattern of cell behavior upon implantation likely to be important for development of the major future body axis. However, the character of these pregastrulation transformations of the egg cylinder has remained unknown. To which extent do they reflect differential growth of the egg cylinder, change in its shape, or cell migration? It has also remained to be determined whether these cell movements that are predictive of anterior-posterior polarity relate to the morphological axes of the embryo, the uterus, or neither.

To approach these questions, we have carried out morphological measurements, gene expression, and cell lineage studies to examine the dynamics of the relationship between the axes of the embryo and the uterus between implantation and gastrulation and their relationship with the molecular emergence of the anterior-posterior axis. This has brought us unexpected insights into the establishment of the anterior-posterior axis in the mouse.

Results

The Embryo Undergoes Dynamic Changes in Its Shape and Orientation with Respect to the Uterus between Implantation and Gastrulation

We first sought to determine the extent to which the morphological axes of the embryo relate to the axes of the uterus shortly after implantation. To address this question we recovered embryos at the earliest possible postimplantation stage (E5.0) up to the time of gastrulation (E6.5) and determined first the extent to which the embryonic region of the developing egg cylinder departed from radial symmetry. At E5.0, each embryo is contained within a crypt, so that the proximal-distal axis of the embryo is parallel to the mesometrial-antimesometrial axis of the uterus (Figure 1A, also [22]). The average proximal-distal length of the embryos at this stage was of 124 $\pm$ 13 μm. Optical sectioning orthogonal to the proximal-distal axis (Figure 1B) revealed that E5.0 embryos were not radially symmetrical but were bilaterally symmetrical, i.e., flattened, such that the short axis was approximately 18% shorter than the long one (74 $\pm$ 5μm compared to 90 $\pm$ 5 μm; n = 14) (Figure 1C). At E5.5, embryos were less flattened and their short axis was only about 5% shorter than the long one (n = 14). Since the average length of the long embryonic axis was relatively unchanged between E5.0–E5.5, it appeared that this shape change was due primarily to an increase in length of the short axis (Figure 1C). By E5.75, cavitation has occurred within the epiblast and a single-layered ectoderm has formed. At this stage, flattening of the embryo reappeared: on average the short axis was 88% of the length of the long one (n = 16). From E5.75–E6.5, the majority of embryos remained ellipsoidal in shape, and as they developed, their flattening became increasingly marked such that by E6.5 one axis was 67% of the length of the other (n = 18) (Figure 1C).

To address whether the orientation of the ellipsoidal-shaped embryos bears any consistent relationship to the axes of the uterus, we performed measurements of histological sections of whole deciduae. This revealed that at E5.0 the embryo's long axis lay almost parallel to the long axis of the uterus displaced only by an average angle of 6° $\pm$ 4° (n = 10) (Figure 2A). At E5.5 it was not possible to orient the embryos, as they had become almost radially symmetrical by this stage. However, at E5.75–E6.0, the long axis of the embryo clearly did not show any specific orientation with respect to the axes of the uterus (Figures 2B and 2C). The mean angle between the long axis of the embryo and the long axis of the uterus was 53° $\pm$ 21°(n = 13) at E5.75 and 52° $\pm$ 26° (n = 30) at E6.0. As embryos developed toward gastrulation their long axes became progressively aligned more perpendicular to the long axis of the uterus. The average angle between the long axis of the embryo and long axis of the uterus was 71° $\pm$ 18° (n = 9) at E6.25 and 74° $\pm$ 13° (n = 12) at E6.5.

In conclusion, E5.0 embryos bear a marked bilateral symmetry and their long axis is oriented parallel to the long axis of the uterus. This bilateral symmetry is, however, transient as the embryos become nearly radially symmetrical at E5.5. As development proceeds to the gastrula stage, flattening of embryos reappears. Initially, however, the embryo's long axis is oriented randomly with respect to the uterine axes. Only shortly before gastrulation does the long axis of the embryo become progressively oriented with respect to the uterine axes. But in contrast to the initial arrangement, at the time of gastrulation, the long embryonic axis adopts a position almost perpendicular to the long axis of the uterus (as also observed in [17, 22]).

Emergence of the Anterior Does Not Correlate with the Uterine Axes but Tends to Correlate with the Morphology of the Embryo

Between E5.5–E6.0, distal visceral endoderm cells move up one side of the embryo to specify the future anterior [7]. Our findings demonstrated that at the time of this movement (E5.75), the morphological axes of the embryo and of the uterus are not in alignment. This raised the question of whether the distal-to-anterior cell movement occurs in a random direction or with respect to an axis of either the uterus or the embryo.

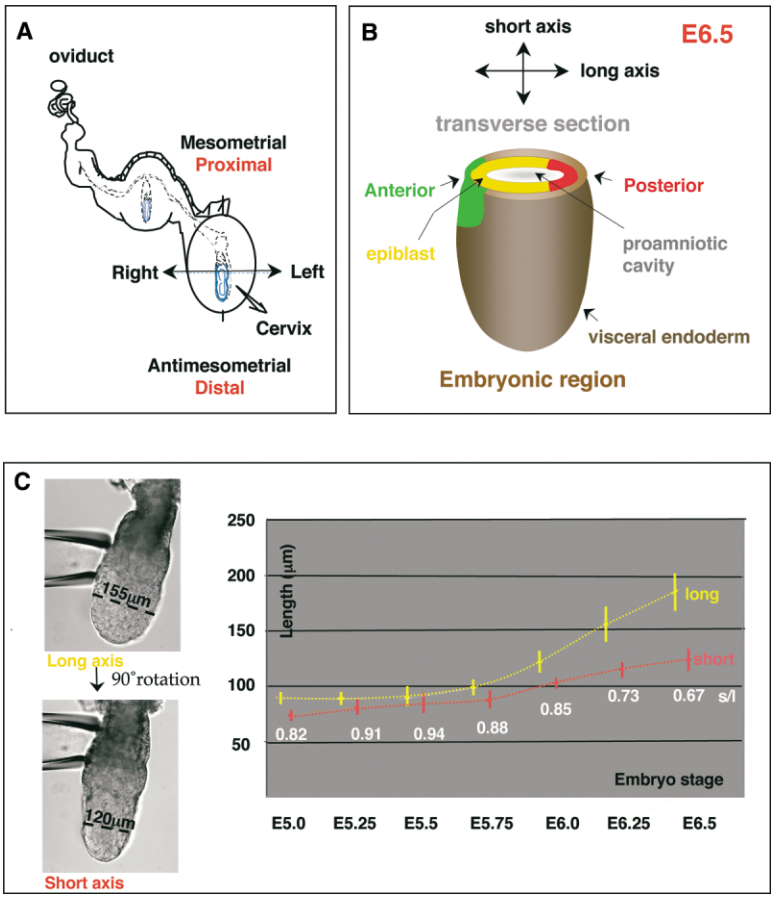

Figure 1. Morphological Axes of the Mouse Egg Cylinder between E5.0–E6.5

(A) Diagram representing the implanted embryo within the uterus at E5.0. The uterine and embryonic axes are shown in black and red, respectively.

(B) A schematic drawing of the embryonic part of the mouse egg cylinder. Arrows indicate short and long embryonic axes and their relationship with the anterior-posterior axis at the time of gastrulation (E6.5). Tissues composing embryonic part of the egg cylinder are also indicated.

(C) Left, two images of an E6.25 embryo oriented through rotation in order to measure its long axis (l, yellow) and short axis (s, red) (black line) that is visible at the embryonic region of the egg cylinder. Right, graph plotting the measurements ±SD of the short (pink line) and long axis (beige line) of the embryo from E5.0–E6.5. The ratio of short axis to long axis (white) is indicated under the paired values. The mean values are shown.

Approaching such a question could be aided by having a marker for the developing AVE that could be observed in both fixed and live preparations. In part to satisfy this need we developed a transgenic line of embryos in which the expression of GFP is driven by the AVE specific *Cerl* gene promoter (*Cerl*-GFP). We then analyzed the pattern of expression of *Cerl*-GFP embryos with respect to the axes of the uterus and the embryo at the time of AVE migration. Comparing the domains of GFP fluorescence with the distribution of *Cerl* mRNA revealed by in situ hybridization confirmed that the GFP expression pattern corresponded to that of endogenous *Cerl* at the time of AVE formation (E5.5–E6.0) (Figures 3A and S1). As expected, GFP expression was observed initially at the distal tip of E5.5 embryos and, within a 6 hr window, it became directed toward one side of the egg cylinder surface. Thus, GFP fluorescence observed in histological sections of *Cerl*-GFP embryos allowed us to follow domains of *Cerl* expression.

To analyze the spatiotemporal expression of *Cerl*-GFP in relation to the axes of the uterus, we fixed whole deciduae when still within the uterus between E5.75–E6.0 and sectioned them for examination by fluorescence microscopy (a typical section is shown in Figure 3B). The pattern of GFP fluorescence was analyzed in each of the sections (of 10 μm thickness). Only the most distal sections were not analyzed (approximately four distal sections, ~40μm) where the GFP-expressing domain could encompass the whole distal visceral endoderm. The position of the domain of GFP-expressing cells was assessed as an angular vector passing through the middle of the arc defined by the GFP domain and originating at the center of the proamniotic cavity. We then classified embryos into three categories (Figure 3C): the "LR" (left or right) category, in which the angle between the vector and the cervix-oviduct axis (α) was between 60°or 90°; the "Ob" (oblique) category, in which the angle was between 30°and 60°; and the "CO" (cervix or oviduct) category, in which the angle was between 0° and 30°. This analysis showed that between E5.75–E6.0, *Cerl* expression was randomly distributed in relation to the uterine axes: 31% (11/36) of embryos were in the CO category, 41% (15/36) of embryos were in the Ob category, and 28% (10/36) of embryos were in the LR category (Figure 3C).

However, we found that the position of GFP expression from the *Cerl* promoter showed a tendency to correlate with the morphology of the embryo. When we related the vector representing the GFP-expressing domain to the morphological long axis of the embryo (Figure 3D), it showed preferential orientation in 51% (21/41) of embryos according to the short embryonic axis (60° to 90°). This compared to 29% (12/41) of embryos, in which it was at an oblique orientation (30° to 60°), and to 20% of embryos (8/41), in which the GFP vector was oriented on the long axis (0° to 30°). Thus, the expression pattern of this marker of AVE formation does not relate to the axes of the uterus before E6.0 but, rather, to the shape of the embryo. However, its relation to the shape of the embryo is not absolute at this

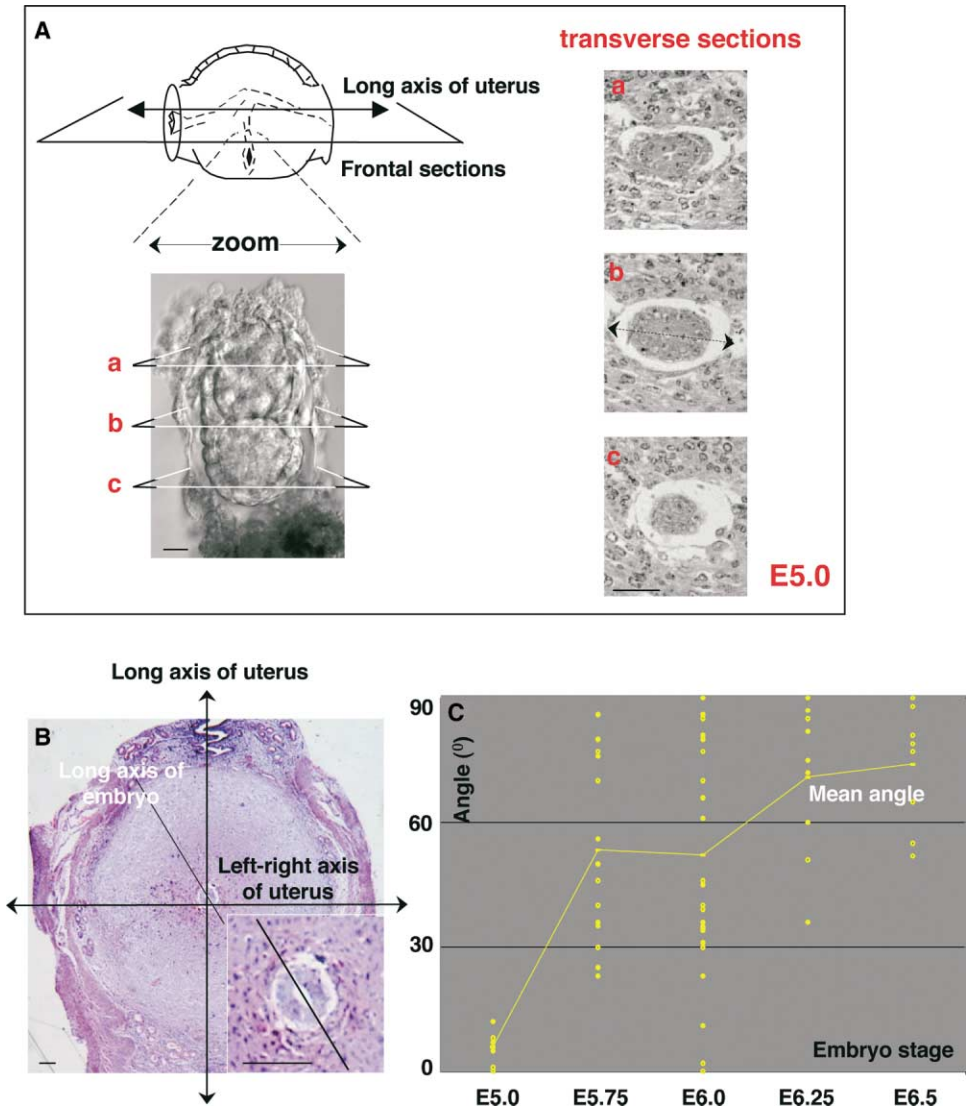

Figure 2. Dynamic Changes in Orientation of the Morphological Axes of the Embryo with Respect to the Uterine Axes

(A) Example of a section of an E5.0 embryo. Frontal sections through the uterus correspond to transverse sections of the embryo. In parts a–c, the horizontal scale bar represents 20 μm. The orientation of each panel bears the same relationship to the axis of the uterus that is indicated in the figure. The long axis of the embryo can be oriented by comparison to the oriented frontal uterine section; a, proximal; b, median; c, distal. The horizontal scale bar represents 50 μm.

(B) A section of the uterus containing an embryo showing embryonic and uterine axes and their relationship. The inset shows a magnified imaged of the same embryo. The horizontal scale bar represents 100 μm.

(C) Plot of the angle between the long axis of the embryo and the long axis of the uterus from E5.0–E6.5. Each yellow dot represents the orientation of the long axis from a single embryo. The line connects the mean angular values.

stage. It seems unlikely that the position of expression of this anterior marker could be an artifact of sectioning since when embryos were removed from uterus and sectioned optically (see Figure S1 for an example of such embryos), expression of the AVE marker was also seen on the short axis at E6.0.

The Emerging Anterior-Posterior Axis Is Initially Not Aligned with the Long but, Rather, with the Short Morphological Axis of the Embryo

The above observations demonstrate, quite unexpectedly, that when the AVE cells move toward the future anterior, they tend not to lie on the long axis of the embryo. This raises the question of how the AVE ultimately becomes positioned so that it does lie on one end of the long axis of the embryo at the time of gastrulation.

To approach this question, we first wished to analyze the expression pattern of not only an anterior marker (*Cerl*), but also posterior markers (*Fgf8* [23] or *Gsc* [24]) in relation to the morphology of the embryo between E6.25–E6.75. In this series of experiments, we turned to using in situ hybridization as it allowed us to follow the position of cells expressing both of these markers. This technique also offers the advantage of providing a closer link to the transcription of the anterior markers as the embryo approaches E6.5 than GFP fluorescence. This

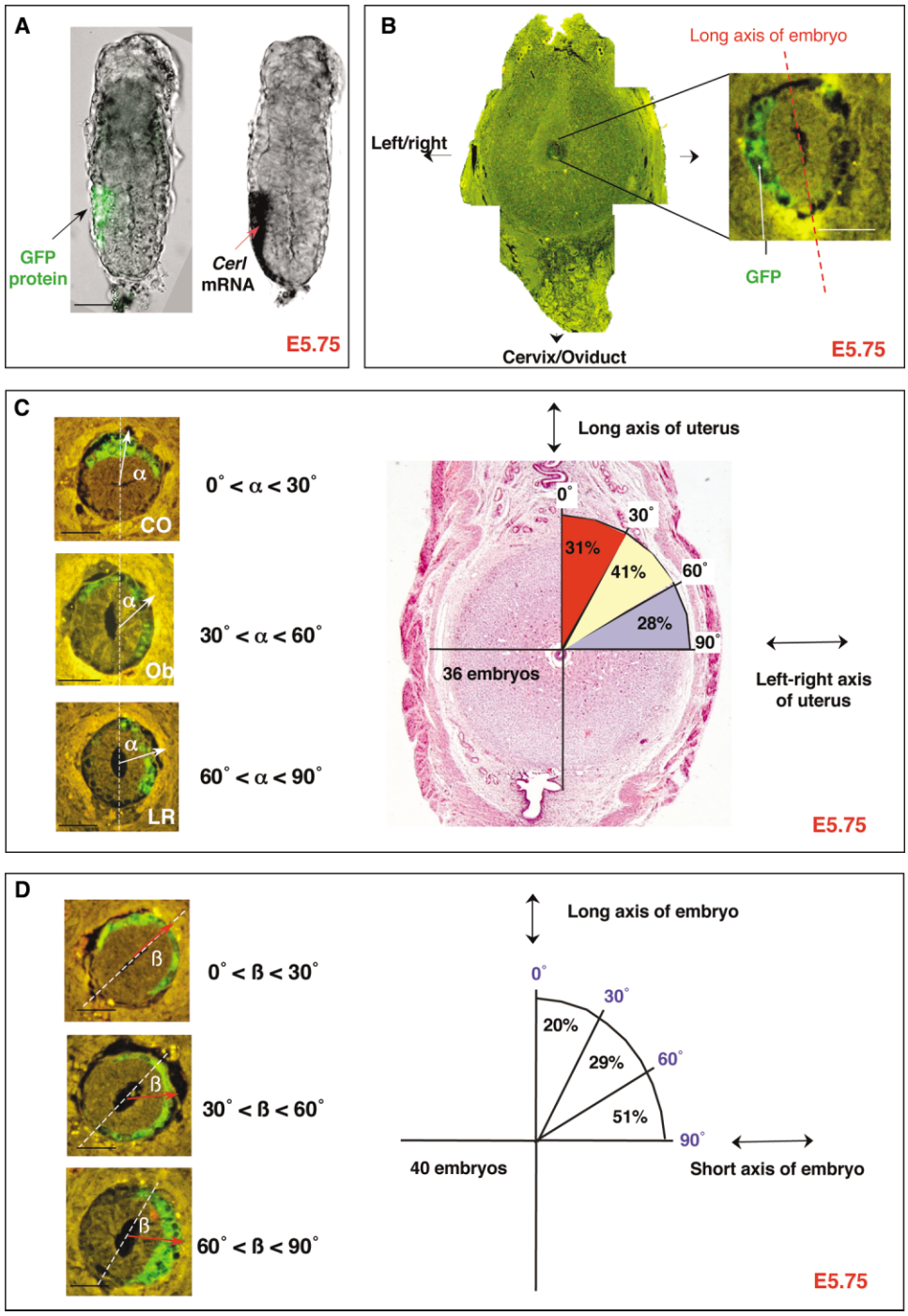

Figure 3. Position of Developing AVE Relates to Embryonic Shape Rather Than to Uterine Axes

(A) GFP fluorescence (left) and in situ hybridization (right) as a marker for *Cerl* expression in the same E5.75 *Cerl*-GFP embryo.

(B) Transverse paraffin section (at lower and higher magnification) of an E5.75 embryo scanned for GFP fluorescence. Note that the GFP protein is specifically localized within the visceral endoderm and remains as a coherent patch.

(C) AVE orientation with respect to the uterine axes was categorized into three distinct groups (CO, Ob, LR) accordingly to the angle (white arrow) between GFP expression domain in relation to the long axis of the uterus. The section only provides visual support to exemplify each different category. In fact, the analysis took all sections into account, so that the final vector represents the average localization of the GFP domain with respect to either the axes of the uterus or the axes of the embryo (Experimental Procedures). Distribution of embryos in each category is indicated.

(D) Three categories of AVE (marked by *Cerl*-GFP expression) orientation (red arrow) with respect to the long morphological axis of the embryo. Ratios of number of embryos in these groups are indicated schematically. All horizontal scale bars represent 50 μm.

is because GFP is quite a stable protein that could, as embryos develop, also effectively act as a lineage tracer of cells expressing the transcript at earlier stages. Indeed, we observed that the domain of expression of *Cerl* mRNA is smaller and contained within the domain marked by *Cerl*-GFP fluorescence at E6.25 and subsequent stages. This suggests that some repression of *Cerl* transcription must operate to restrict expression to a subset of cells within the progeny of the original population of cells that had expressed *Cerl*-GFP. We later confirmed this restriction of expression by marking the boundaries of the GFP-expressing population of cell with DiI at E6.0 and by showing that *Cerl* mRNA was expressed later within a smaller domain (see below).

As expected, we observed that at E6.75, the axis passing through the center of the expression domains of *Cerl* and *Fgf8* (the anterior-posterior axis) was almost parallel to both the long axis of the embryo and the left-right axis of the uterus (Figure 4A). The domains of expression of *Cerl* and *Fgf8* were diametrically opposite to each other (Figure 4A). However, at E6.0–E6.25, the axis defined by the center of the expression domains of both *Cerl* and *Fgf8* tended to be either perpendicular or oblique, rather than parallel, to the embryo's long axis (Figure 4B). This finding is in direct agreement with our previous observations on the pattern of GFP expression from the *Cerl* promoter at E6.0. The slight variability observed in the initial positioning of the anterior-posterior axis in relation to embryo morphology could, perhaps, reflect some variation in the developmental stage of the embryo, which indeed could be recognized by some differences in the sizes of the embryos collected at the same developmental time point (see Figure 1C and Experimental Procedures). These observations might be interpreted as indicating that as development proceeds beyond E6.25 toward E6.5, the axis defined by the center of the expression domains of both *Cerl* and *Fgf8* becomes progressively oriented toward being parallel with the long axis of the embryo. Our results would therefore suggest that this trend in reorienting the anterior-posterior axis in relation to the embryo's morphology could already be seen in some embryos collected at E6.25 (Figure 4C).

A Change in Embryo Shape Appears to Align the Anterior-Posterior Axis with the Long Morphological Axis of the Embryo

Several hypotheses can be put forward to explain how the orientation of the anterior-posterior axis could change with respect to the morphological axes of the embryo (Figure 5A). It could reflect asymmetric cell migration, whereby cells expressing anterior and posterior markers move toward the opposite ends of the long embryonic axis; a change in anterior and posterior gene expression pattern so that expression of the anterior and posterior markers is restricted and maintained only toward the ends of the long axis; or a change in the embryo's shape so that the ends of the short axis become the ends of the long axis. To gain insight into these possibilities, we carried out cell lineage studies to follow development of the anterior-posterior axis from E6.0 in embryos subjected to short-term culture in vitro. To detect de novo *Cerl* expression as a marker of the final position of the AVE, we used in situ hybridization. To detect the original domain of *Cerl* expression, we had to allow for the extensive cell movements that occur in the visceral endoderm of the embryonic region of the egg cylinder at this stage [11]. As a result, not only does GFP expressed from the *Cerl* promoter mark the history in addition to the ongoing expression of *Cerl*, but also the colony of GFP-labeled cells becomes quite scattered around E6.25. Thus, to be able to relate the final position of the AVE (ongoing *Cerl* expression) to its original expression domain at E6.0, we further marked the lateral limits of the domain of cells expressing GFP at E6.0 by labeling cells with DiI (Figure 5B). DiI was applied at two extreme positions on the extraembryonic visceral endoderm cells, close to their embryonic boundary, since cells in this particular region do not undergo the same dramatic movements typical of the embryonic region [11, 25–27]. The labeled embryos were then cultured and allowed to develop for 15–18 hr before analyzing the position of DiI fluorescence in relation to ongoing anterior and posterior gene expression revealed by in situ hybridization for *Cerl* and *Gsc*, respectively. In these experiments, 21 of 33 DiI-labeled prestreak embryos reached the early primitive streak stage in culture as assessed by the expression of the anterior and posterior markers. All of these embryos showed an ellipsoid shape.

The clear finding to emerge from these experiments was that the final position of the AVE was at one end of the long embryonic axis in the great majority (20 out of 21) of embryos. This indicates that the "repositioning" of the AVE toward the end of the long axis can take place in the absence of the uterus. Secondly, the final position of the AVE (as detected by in situ) was always (100%, $n = 21$) found within the domain previously defined by the GFP cells that lay in between the two patches of DiI-labeled cells (Figures 5Ba–5Be). This argues that the AVE does not reform away from its initially determined position during the time of culture in vitro.

Additionally, we attempted to analyze the exact location of the AVE in relation to its earlier position at E6.0 by comparing the site of *Cerl* transcripts within the domain of GFP fluorescence marked by two patches of DiI (Figure 5B). To this end, we divided the intervening region between the two extreme DiI patches into three equal parts (Figure 5C). We found that of 20 embryos in which the AVE became positioned at the end of the long axis at the primitive streak stage, 11 had *Cerl* mRNA within a central sector of the "DiI-defined GFP region." In the remaining nine embryos, it was within one of the lateral sectors of such a region. Ongoing *Cerl* expression in the central part of the DiI-marked region might point to a change in embryo shape as being responsible for bringing the AVE toward the end of the long axis. Alternatively, it might point to an integral movement of the entire *Cerl*-GFP expression domain toward this end. This latter possibility, however, we find very unlikely. This is because had there been an integral movement of the entire *Cerl*-GFP expression domain toward the anterior (end of the long axis), then in contrast to what we observed, its position relative to the DiI labeled cells would have changed. Ongoing expression of *Cerl* toward the edges

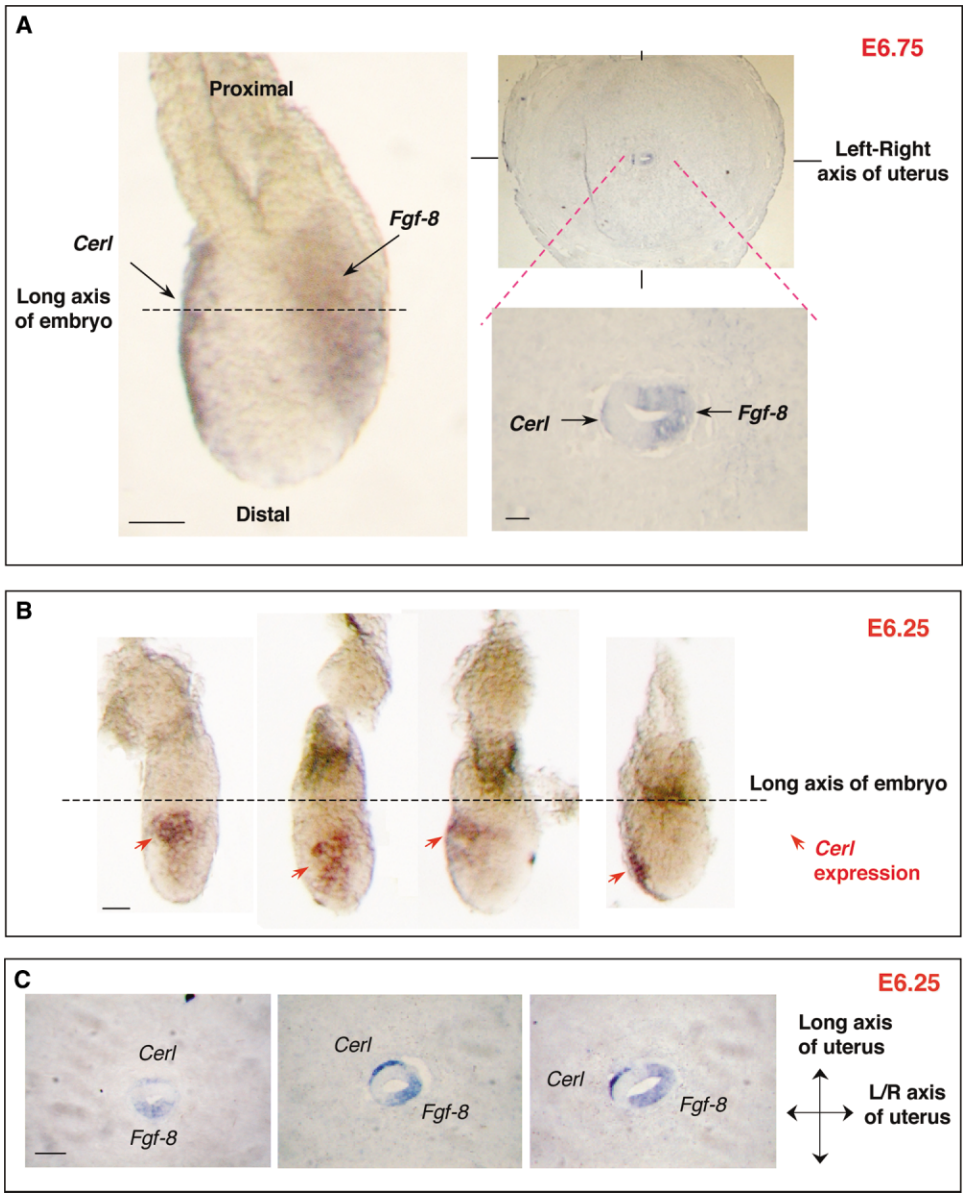

Figure 4. The Anterior-Posterior Axis Changes Its Position with Respect to Morphology of the Embryo between E6.25–E6.75

(A) In situ hybridization for *Cerl* and *Fgf8* expression in an E6.75 embryo. Right reveals in situ hybridization for *Cerl* and *Fgf8 mRNAs* on a paraffin section of the E6.75 decidua at lower (top) and higher (bottom) magnification.

(B) Whole-mount in situ hybridization showing *Cerl* mRNA (red arrows) in four E6.25 embryos. Dotted lines represent the long morphological axis of the embryo.

(C) In situ hybridization for *Cerl* and *Fgf8* on sections of E6.25 decidua. All horizontal scale bars represent 50 μm. All sections are oriented with the long axis of the uterus as indicated.

of the DiI marked region could indicate that the expression of *Cerl* became restricted to one edge of its initial expression domain so that the AVE became positioned closer to the end of the long embryonic axis. But this outcome could also point to the embryo changing its shape, although in this case not symmetrically with respect to the center of the initial domain of anterior marker expression (see also the Discussion section below). A very similar "repositioning" of the anterior-posterior axis in relation to the change in the embryo shape is also reported in Perea-Gomez et al. ([34], this issue of *Current Biology*).

Although at present it is not possible to track a shape change of the embryo as it occurs in utero, perhaps some signs of such a change could be indicated when we sectioned embryos perpendicularly to their proximal-distal axis. We found that E6.25–E6.5 embryos sectioned in this way could appear to be slightly "spiral" in their embryonic regions. The orientation of the long axis of the same embryo as measured in the distal and the proximal regions could differ by up to 28°, although the mean of this difference was only 11.3° for 18 embryos measured (Figure 6).

Taken together, all these results lead us to propose

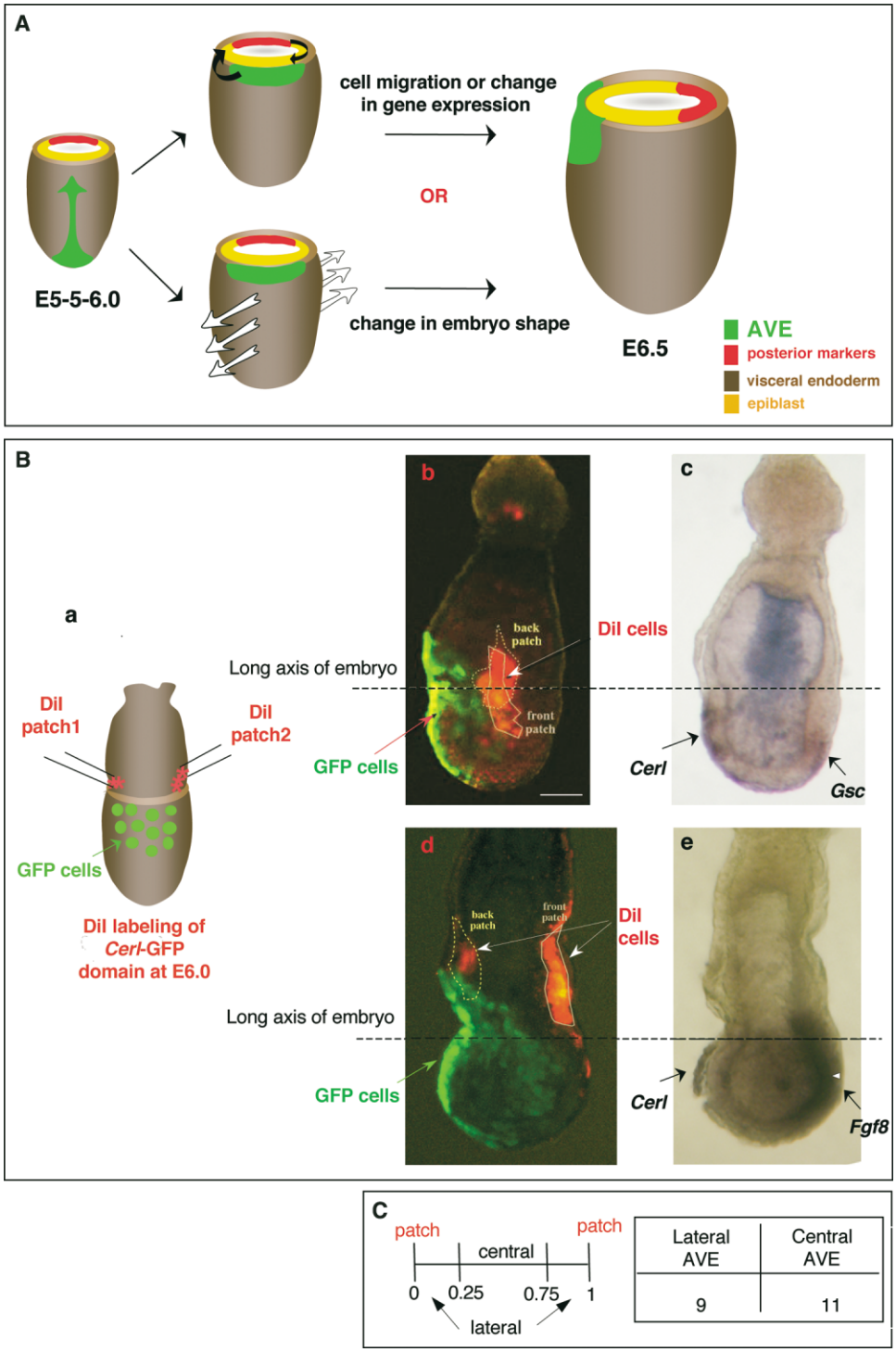

Figure 5. The Apparent Shift of the Anterior-Posterior Poles toward the Opposing Ends of the Long Embryonic Axis Appears to Be Associated with a Change in Embryo Shape

(A) A schematic representation of possible routes whereby the anterior-posterior axis might change its position in respect to the embryo morphological axes between E6.0–E6.5. The AVE (marked by the green arrow) first migrates proximally ("anteriorly") along the short axis of the embryo at E5.5–R6.0. Then, in the first possibility, either cells expressing anterior and posterior markers move toward the ends of the long embryonic axis or there is a restriction in the transcription of anterior and posterior markers so that their expression is maintained only at the ends of the long axis. In the second possible route, the embryo is changing shape so that the ends of the short embryonic axis become the ends of the long axis, possibly by preferential growth of the epiblast and visceral endoderm in the short axis.

(B) In vitro cell lineage studies of AVE position with respect to the embryonic axes. *Cerl*-GFP embryos were collected at E6.0, and both lateral groups of cells expressing GFP were labeled with DiI (a). At E6.0 the domain of *Cerl* expression revealed by GFP fluorescence and by in situ hybridization colocalize (see Figure S1). Labeled embryos were cultured for 15–18 hr and analyzed by fluorescence microscopy to reveal the

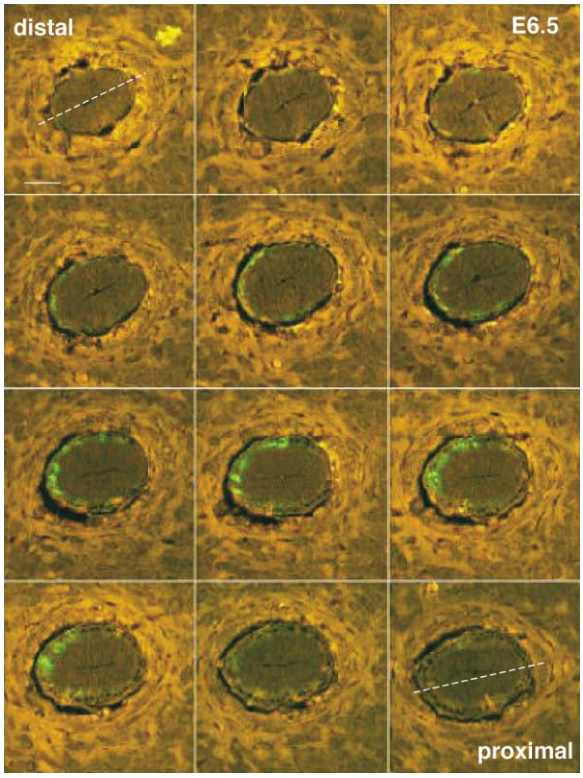

Figure 6. Change in Shape of the Embryonic Region of the Egg Cylinder along Its Proximal-Distal Axis at E6.5

Series of paraffin sections of a single E6.5 embryo expressing *Cerl*-GFP in utero. The orientation of the long axis of the embryo (marked by the white dashed line) can slightly differ at the distal and proximal parts of the embryonic region of the egg cylinder (the mean of this difference being 11.3° for 18 embryos measured). The horizontal scale bar represents 50 μm.

that the mouse embryo changes its shape shortly before gastrulation and that the extent to which the shape is changed might slightly differ and so be characteristic for individual embryos. We think that such a shape change could be accompanied by the fine-tuning of the expression of anterior and posterior markers so that ultimately the AVE is positioned toward the end of the long embryonic axis at the time of gastrulation (Figure 7). In the case of *Cerl*, this is seen as a restriction of its transcription within a subset of cells of those originally expressing the protein.

Discussion

We describe here three major shape changes that take place in the mouse embryo in the interval between implantation and gastrulation. The embryo is flattened at implantation and then becomes almost radially symmetrical about its long axis. It subsequently undergoes flattening again from E5.5 onward, a time when the distal tip cells are migrating to their anterior destination. The third change, immediately before gastrulation, is an adjustment in both shape and gene expression that places the long axis of the embryo in register with the anterior-posterior axis and the left-right axis of the uterus. A model of how these changes in embryo shape might take place in relation to the orientation of the anterior-posterior axis and the axis of the uterus is presented in Figure 7.

It is not yet clear how the flattening of the embryo at the time of implantation relates to formation of the anterior-posterior axis. The flattening we observe at E5.0 may correspond to the bilateral symmetry ascribed by Smith [16, 17] to the implanting blastocyst. Smith suggested that the asymmetries she saw, which related to the blastocyst axis of bilateral symmetry, may also be directly related to the final orientation of the anterior-posterior axis. However, the complexity of cell movement and growth from the blastocyst to the early egg cylinder stage revealed by our previous studies [11] indicated that this relationship might not be so straightforward. Although we observed that the visceral endoderm progeny of inner cell mass cells from the ends of the blastocyst axis of bilateral symmetry tended to differ in their spatial distribution along the proximal-distal axis of the egg cylinder, they did not occupy exclusively anterior or posterior positions. We believe that it is difficult at present to relate these findings to each other since we do not yet know how bilateral symmetry before implantation relates to that after implantation and in turn to that of the E5.0 egg cylinder of this study. Our present data add a further complication that should be taken into account in understanding the relationships between morphology of the embryos at different stages of the peri-implantation development on one hand and the emergence of the anterior-posterior axis on the other. This is that the embryo passes through an intermediate stage that approaches radial symmetry around the time when the anterior-posterior axis can be described by current molecular markers, and we have no molecular markers at these earlier stages to which the shape changes can be referred. We can, however, hypothesize in relation to the present data about the nature of the mechanisms that link subsequent changes in the embryo shape to the molecular specification of the emerging anterior-posterior axis. It is possible that flattening at the time of the distal-to-anterior cell movement arises as a result of the mode of the growth of the egg cylinder. The distal-to-anterior migration would then be a natural extension of this growth pattern. Our data do not, however, allow us to exclude that the flattening of the embryo might also partly be a consequence of this cell migration per se. This second hypothesis seems to be favored in a recent study by Rivera-Perez and colleagues (published

position of DiI- and GFP-expressing cells (b and d). The same embryos were subsequently processed through in situ hybridization to detect the expression of *Cerl* and *Gsc* or *Fgf8* (c and e). The horizontal scale bar represents 50 μm.

(C) The position of the AVE (indicated by the in situ hybridization for *Cerl*) was then scored, according to its localization with respect to the two lateral patches of DiI, as central or lateral. The accompanying table shows the distribution of AVE with respect to the patches of DiI in cultured embryos.

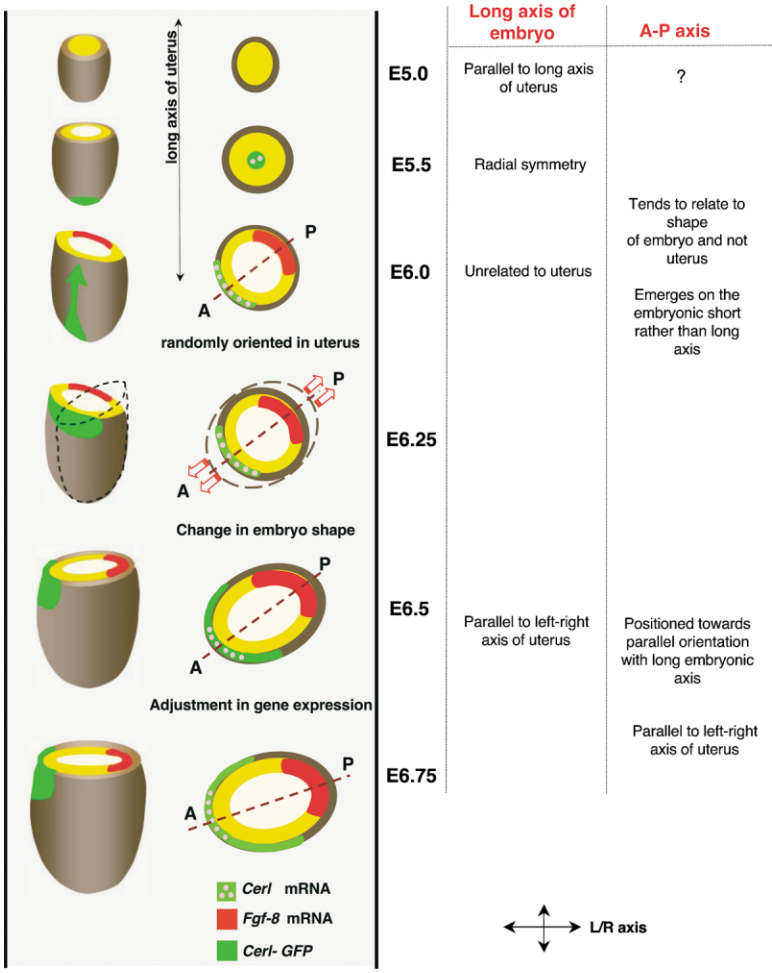

Figure 7. Development of the Anterior-Posterior Axis in the Embryo Implanted in the Uterus

Schematic representation of the dynamic relationship between the axes of the embryo and anterior-posterior axis on one hand and the axes of the uterus on the other hand from E.5.0–E6.75. Schematic drawings of the embryonic region of the egg cylinder (left) and its transverse sections (right) as they develop within the uterine wall (gray). At E5.0, the long morphological axis of the flattened embryo is aligned with the long axis of the uterus. This bilateral symmetry is lost by E5.5 and then regained with the embryo becoming randomly orientated within the uterine wall at E5.75 until shortly before gastrulation. The emergence of the anterior-posterior axis, first visualized as distal-to-anterior movement of visceral endoderm cells that takes place between E5.5–E6.0, occurs during the period that the embryo is randomly oriented. The anterior-posterior axis tends to emerge with respect to the morphology of the embryo and not the uterus. However, the initial position of the anterior-posterior axis does not correspond to the long axis of the embryo, whereas half a day later it will do so. Our results suggest that this apparent "shift" in orientation of the anterior-posterior axis results from a change in the shape of the embryo. This change in shape can be associated with some adjustment of gene expression patterns that ultimately will relate the orientation of the anterior-posterior axis with the axes of the uterus. This suggests a fine interdependence between the expression of anterior-posterior markers, the shape of the embryo, and the axes of the uterus.

during revision of our paper), showing that the epiblast facing the AVE is flattened at the time when it migrates anteriorily [27]. However, neither this nor our own study addresses whether the embryo flattening is the cause or the consequence of AVE formation.

Studies of cell lineages carried out in vitro by us in this paper and also by Perea-Gomez and colleagues [34] suggest that the AVE (and/or posteriorly expressed genes) is able to direct formation of the future long axis of the embryo. However, we have shown that neither the AVE nor the long axis of the embryo is related to any specific uterine axis at E6.0. This therefore implies that both the AVE and the uterus direct formation of the long axis of the embryo in such a way that it is aligned with them. Further analysis will be required to characterize morphogenetic movements together with molecular contributions in order to understand the fine interplay between these three partners.

The repositioning of the long axis of the embryo and the anterior-posterior axis to eventually align occurs both in embryos developing in utero and in vitro. We hypothesize that this alignment is likely to be due to a change in shape caused by the preferential growth of epiblast and visceral endoderm along what at E6.0 is the short axis; this expanded tissue would then form part of the ends of the long axis as seen at gastrulation (Figure 7). Our lineage tracing experiments demonstrate that the domain of expression of the AVE marker *Cerl* becomes restricted at this stage in a manner that varies from one embryo to another. This slight variability in the position of ongoing *Cerl* expression within the DiI-marked region at E6.5 may reflect the extent to which its expression naturally fell toward the end of the long rather than the short axis at E6.0. In such a case, there would be little requirement for any later readjustment of the expression domain. If at E6.0, *Cerl* expression tended to occur on the short axis, there would be a greater need for the expression domain to reposition and so compensate. This would ensure that the AVE ultimately lies on one end of the long axis. Thus, this change in embryo shape before gastrulation might be understood as providing an important link to axis specification by positioning the anterior and posterior ends farthest apart from each other, thus toward the ends of the long rather than the short axis. Anterior and posterior poles would then tend to become more focused at the opposing positions on the narrowmost parts of the egg cylinder but maintained apart due to a system of repression. Such, still hypothetical behavior of anterior and posterior poles would be in agreement with the recently proposed models [12, 14] in which the AVE acts by suppressing and restricting the posteriorizing signals,

becoming necessary to segregate the anterior and the posterior "organizing" centers to achieve a correct patterning of the early gastrula embryo.

The fact that embryos cultured in vitro are not in their normal environment and still undergo these changes offers some additional insight into development of the anterior-posterior axis. It suggests that the apparent repositioning of the anterior-posterior axis can occur independently of the uterus. If the embryo does indeed have some intrinsic potential to position its anterior-posterior axis, where could this potential positional information come from? One possibility is that it might relate to the bias in polarity of the embryo that develops at the preimplantation stages [11, 19–21, 28–31]. However, although the embryo might have the intrinsic potential to position the anterior-posterior axis, a role for the uterus cannot be fully excluded, either earlier in determining the extent of embryo flattening and/or later in fixing the final orientation of the anterior-posterior axis. Indeed a mechanism must exist for the embryo to become aligned with respect to the uterine axis from the time of gastrulation. Is the uterus imposing this final alignment through the remodeling of the embryo? Or has some intrinsic information been fixed in the embryo with reference to the uterus from the time of implantation? These questions remain open. In order to fully understand the changes in embryo shape and cell movements implicit from these studies and also from our previous work [11], time-lapse observations of egg cylinder transformations after implantation would be most helpful, ideally in utero, but most likely achievable following short-term culture in vitro.

Conclusions

At the time of distal-to-anterior visceral endoderm cell migration, the morphological axes of the mouse embryo are not aligned with those of the uterus. Development of the anterior-posterior axis tends first to relate to the shape of the embryo and not to the axes of the uterus. A change in embryo shape together with fine-tuning in the expression of the anterior and posterior markers just before gastrulation aligns the long axis of the embryo with its anterior-posterior axis. This occurs in concert with an alignment of the embryo with the uterine axes.

Experimental Procedures

Embryos

F1 (C57BL6 × CBA) or C*erl*-GFP transgenic mice (see below) were bred with artificial "day/light" being maintained from 06:00–18.00 hr. All of the analyzed embryos or deciduae were obtained from naturally mated F1 × F1 or F1 female × C*erl*-GFP male crosses. They were staged according to the time of recovery as follows. E5.0 for embryos that were recovered between 21:00–03:00 hr on the fourth to fifth day after fertilization (day of plug), E5.25 between 03:00–09:00 hr on the fifth day, E5.5 between 09:00–15:00 hr on the fifth day, E5.75 between 15:00–21:00 hr on the fifth day, E6.0 between 21:00–03:00 hr on the fifth to sixth day, E6.25 between 03:00–09:00 hr on the sixth day, E6.25 between 09:00–15:00 hr on the sixth day, and E6.75 between 15:00h-21:00h of the 6th day. The average proximal-distal length of the embryos at stages between E5.0–E6.5 was E5.0, 124 ± 13 μm (n = 14); E5.25, 167 ± 22 μm (n = 9); E5.5, 185 ± 15 μm (n = 16); E5.75, 202 ± 29 μm (n = 14); E6.0, 248 ± 37 μm (n = 14); E6.25, 324 ± 23 μm (n = 12); and E6.5, 340 ± 31 μm (n = 17). See also data showing the average diameter of the embryonic portion of the egg cylinder throughout these stages (Figure 1C).

Generation of *Cerl*-GFP Transgenic Embryos

To generate embryos that express GFP from the *Cerberus-like* promoter, an EcoRI genomic fragment containing the first exon of *Cerl* gene and 4 kb of noncoding upstream region was isolated from a mouse genomic library generated in Lambda Fix II (Stratagene) and subcloned into pBluescriptIIKS+ (Stratagene). An NcoI site was introduced at the starting ATG codon by PCR-based mutagenesis. To generate the plasmid *Mcerl*P-EGFP a 1 kb NcoI–SspI fragment containing the enhanced green fluorescence rrotein (EGFP) CDS and the SV40 early mRNA polyadenylation signals from pEGFP-N3 (Clontech) was inserted at the *Cerl* ATG site.

The transgenic line TgN(CerlPGFP)328Belo (referred to in the text as *Cerl-GFP*) was generated by microinjection of a BssH fragment from *Mcerl*P-EGFP into the pronuclei of fertilized eggs from C57/Bl6 mice, as described [31]. Genotyping was carried out by PCR analysis of adult tail DNA using oligonucleotides 5′-GACGAATT CACCCACCTGCTGACCACCTGCTTCC-3′ and 5′-TTGATGCCGTT CTTCTGCTTGTCG-3′, which amplify a 600 bp transgene-specific product.

Measurements of Embryonic Dimensions

Embryos were orientated using a holding pipette and a micromanipulator over an inverted microscope (Nikon). They were rotated along their proximal-distal axis to observe their short and long axis of bilateral symmetry. Measurements were carried out on the photographs (CCD camera, Princeton Instruments) taken with the optical section passing through the central thickest part of the embryo, where the axis was the longest. The real dimensions of the embryo were adjusted according to the magnification used (10×, 20× lens). Measurements were taken at an embryonic region of the egg cylinder, two-thirds from the distal tip. Throughout the text, we refer to the morphological axes of the embryonic region of the egg cylinder when it is flattened as the long or short axis of the embryo.

To relate the axes of the embryo to the uterus, the former were first determined by examining the shape of the decidua at low magnification (5–10×); the axes of the embryo were then determined under high magnification (40×), and both sets of axes were compared to each other. In the few cases where the long axis of the embryo was not obviously identifiable, the long proamniotic axis could still be used as a reference. Indeed, in this study it systematically appeared to be parallel to the long axis of embryo bilateral symmetry.

Whole-Mount In Situ Hybridization

Embryos were recovered in M2 medium and fixed in 4% paraformaldehyde in PBS at 4°C. In situ hybridizations using digoxigenin-labeled probes were performed as described by Wilkinson [32], modified by the omission of proteinase K treatment. All digoxigenin-labeled antisense probes were hybridised at 65°C for 12–20 hr. The probes used in this study corresponded to the following genes: *Fgf8*, *Cerl*, *Gsc*, and *T* [33]. For in situ hybridization on histological sections, the sections were dewaxed and rehydrated before immediately undertaking in situ hybridization protocol. The same procedure was applied except that a proteinase K (10 μg/μl) treatment was included for 10 min followed by postfixation in 4% paraformaldehyde for 10 min.

Embedding for Histological and GFP Analysis of *Cerl-GFP* Embryos

Deciduae were recovered at the indicated stages in M2 medium or PBS and fixed immediately in 4% paraformaldehyde overnight at 4°C. They were washed twice for 10 min in PBS and processed through ethanol dehydration for successive periods of 10 min in 25%, 50%, 75%, 90%, and 96% ethanol in PBS. Subsequently, they were kept in 96% ethanol (for up to 1 day), transferred to 1:1 ethanol:xylene for 1 hr, then to 1:1 xylene:Paraplast plus wax (Sigma) for 1 hr at 65°C, and finally twice to wax for 1 hr at 65°C. For final embedding, they were oriented with the mesometrium-antimesometrium axis vertical in a 8 mm^3 cubic chamber and maintained at 4°C until sectioning. Sections were cut at 10 μm and laid on APES- or polylysine-coated slides when required for in situ hybridization. For

histological analysis, sections were stained with Ehrlich's Haematoxylin and Eosin and mounted under a glass coverslip with DPX (BDH).

Confocal Microscopy

Dissected embryos were fixed in 4% paraformaldehyde, transferred, and oriented in a glass-bottomed coverslip dish in PBS before scanning. To detect GFP expression, sections were kept in wax and directly scanned. Laser scanning confocal microscopy was carried out on an inverted Nikon microscope with a Biorad MRC Scanning head.

Vector Analysis

For each section within the same embryo, except the very distal ones (-40 μm), a vector was determined representing the median orientation of the GFP expression domain as well as its expanse. An angular frame of reference was defined, with the origin being at the intersection between the minor and the major axes of the embryo and with an axis of reference, the x axis, arbitrarily fixed. The vector was empirically traced, starting at the origin of the angular frame of reference and passing by the middle of the arc defined by the GFP-expressing cells (the bisecting line). The value of the radial distance to the origins, r_i, was determined by the length of the same arc. The angle between the vector and the x axis, θ_i, was then calculated with the help of a protractor and respecting the trigonometric direction, i.e., clockwise. By that way a vector, v_i, was finally defined with the polar coordinates (r_i, θ_i). In Cartesian coordinates, this corresponds to $v_i = r_i$ ($\sin\theta_i$ x + $\cos\theta_i$ y). The global median resulting vector, V_r, was calculated by vector addition of the total number of vectors, n: $V_r = (v_1 + v_2 + \ldots + v_i + \ldots + v_n)/n = ax + by$ (a and b being the Cartesian coordinates). The Cartesian coordinates (a, b) were then converted into polar coordinates (r_r, θ_r), θ_r then being the resulting angle that the radial line of the overall resulting vector makes with the axis of reference, the x axis.

DiI Labeling

Cerl-GFP embryos were recovered between 00:00–05:00 hr on the sixth day after the day of fertilization in M2 medium supplemented with 10% fetal calf serum (FCS). The Reichert's membrane was punctured to release the embryo. Embryos were labeled with 0.05% DiI in 0.3 M sucrose and 5%–20% ethanol using a Leica micromanipulator and microscope. Embryos were oriented during a short exposure to blue light to reveal GFP fluorescence. Micromanipulation needles were back filled with about 10 nl of the DiI solution, and the tip was cut to have a diameter of about 5–10 μm. Labeling was performed by apposing the tip very close to the selected GFP-positive cells and expelling some of the solution using an oil pump while then moving proximally along the proximal-distal axis. The labeled region was a line of one to two cells wide, spanning a region from above the embryonic-extraembryonic junction and comprising the lateral edge of the GFP positive region. The labeling position was verified by short exposure to reveal both green and red fluorescence. Embryos were washed in 1:1 DMEM:FCS and transferred to 1:1 DMEM:rat serum for 15–18 h of static culture in 5% CO_2 at 37°C. Embryos were fixed in 4% paraformaldehyde, laid on their short axis of bilateral symmetry, and scanned by confocal microscopy to reveal GFP and DiI. Embryos were then processed through the in situ hybridization protocol to localize expression of the markers *Cerl* and *Gsc* or *Fgf8* to assess their development and confirm the position of the anterior-posterior axis.

Supplemental Data

Supplemental Data including a figure showing colocalization of GFP and mRNA Expression from the *Cerl* promoter are available at http://www.current-biology.com/cgi/content/full/14/3/184/DC1/.

Acknowledgments

This work was supported by the Wellcome Trust Senior Research Fellowship to M.Z.-G., and by F.C.T. and IGC/Fundação Calouste Gulbenkian to J.A.B. D.M. and M.F. were supported by PhD studentships from the Biotechnology and Biological Science Research Council and F.C.T, respectively. We thank Maria Elena Torres Padilla, David Glover, Patrick Tam, Claudio Stern, and Stephen Frankenberg for the discussions. We also thank Aitana Perea-Gomez and Jérôme Collignon for sharing their results with us before publication and for discussions.

Received: August 20, 2003
Revised: December 24, 2003
Accepted: December 30, 2003
Published: February 3, 2004

References

1. Lu, C.C., Brennan, J., and Robertson, E.J. (2001). From fertilization to gastrulation: axis formation in the mouse embryo. Curr. Opin. Genet. Dev. *11*, 384–392.
2. Lawson, K.A., Dunn, N.R., Roelen, B.A., Zeinstra, L.M., Davis, A.M., Wright, C.V., Korving, J.P., and Hogan, B.L. (1999). Bmp4 is required for the generation of primordial germ cells in the mouse embryo. Genes Dev. *13*, 424–436.
3. Varlet, I., Collignon, J., and Robertson, E.J. (1997). Nodal expression in the primitive endoderm is required for specification of the anterior axis during mouse gastrulation. Development *124*, 1033–1044.
4. Brennan, J., Lu, C.C., Norris, D.P., Rodriguez, T.A., Beddington, R.S., and Robertson, E.J. (2001). Nodal signalling in the epiblast patterns the early mouse embryo. Nature *411*, 965–969.
5. Liu, P., Wakamiya, M., Shea, M.J., Albrecht, U., Behringer, R.R., and Bradley, A. (1999). Requirement for Wnt3 in vertebrate axis formation. Nat. Genet. *22*, 361–365.
6. Thomas, P.Q., Brown, A., and Beddington, R.S. (1998). Hex: a homeobox gene revealing peri-implantation asymmetry in the mouse embryo and an early transient marker of endothelial cell precursors. Development *125*, 85–94.
7. Thomas, P., and Beddington, R. (1996). Anterior primitive endoderm may be responsible for patterning the anterior neural plate in the mouse embryo. Curr. Biol. *6*, 1487–1496.
8. Belo, J.A., Bouwmeester, T., Leyns, L., Kertesz, N., Gallo, M., Follettie, M., and De Robertis, E.M. (1997). Cerberus-like is a secreted factor with neutralizing activity expressed in the anterior primitive endoderm of the mouse gastrula. Development *68*, 45–57.
9. Biben, C., Stanley, E., Fabri, L., Kotecha, S., Rhinn, M., Drinkwater, C., Lah, M., Wang, C.C., Nash, A., Hilton, D., et al. (1998). Murine cerberus homologue mCer-1: a candidate anterior patterning molecule. Dev. Biol. *194*, 135–151.
10. Shawlot, W., Deng, J.M., and Behringer, R.R. (1998). Expression of the mouse cerberus-related gene, Cerr1, suggests a role in anterior neural induction and somitogenesis. Proc. Natl. Acad. Sci. USA *95*, 6198–6203.
11. Weber, R., Wianny, F., Evans, M., Pedersen, R., and Zernicka-Goetz, M. (1999). Polarity of the mouse embryo is anticipated before implantation. Development *126*, 5591–5598.
12. Kimura, C., Yoshinaga, K., Tian, E., Suzuki, M., Aizawa, S., and Matsuo, I. (2000). Visceral endoderm mediates forebrain development by suppressing posteriorizing signals. Dev. Biol. *225*, 304–321.
13. Kimura, C., Shen, M.M., Takeda, N., Aizawa, S., and Matsuo, I. (2001). Complementary functions of Otx2 and Cripto in initial patterning of mouse epiblast. Dev. Biol. *235*, 12–32.
14. Perea-Gomez, A., Vella, F.D., Shawlot, W., Oulad-Abdelghani, M., Chazaud, C., Meno, C., Pfister, V., Chen, L., Robertson, E., Hamada, H., et al. (2002). Nodal antagonists in the anterior visceral endoderm prevent the formation of multiple primitive streaks. Dev. Cell *25*, 745–756.
15. Ding, J., Yang, L., Yan, Y.T., Chen, A., Desai, N., Wynshaw-Boris, A., and Shen, M.M. (1998). Cripto is required for correct orientation of the anterior-posterior axis in the mouse embryo. Nature *395*, 702–707.
16. Smith, L.J. (1980). Embryonic axis orientation in the mouse and its correlation with blastocyst relationships to the uterus. Part 1. Relationships between 82 hours and 4 1/4 days. J. Embryol. Exp. Morphol. *55*, 257–277.
17. Smith, L.J. (1985). Embryonic axis orientation in the mouse and

its correlation with blastocyst relationships to the uterus. II. Relationships from 4 1/4 to 9 1/2 days. J. Embryol. Exp. Morphol. *89*, 15–35.

18. Tam, P.P., Gad, J.M., Kinder, S.J., Tsang, T.E., and Behringer, R.R. (2001). Morphogenetic tissue movement and the establishment of body plan during development from blastocyst to gastrula in the mouse. Bioessays *23*, 508–517.
19. Zernicka-Goetz, M. (2002). Patterning of the embryo: the first spatial decisions in the life of a mouse. Development *129*, 815–829.
20. Gardner, R.L. (1997). The early blastocyst is bilaterally symmetrical and its axis of symmetry is aligned with the animal-vegetal axis of the zygote in the mouse. Development *124*, 289–301.
21. Ciemerych, M.A., Mesnard, D., and Zernicka-Goetz, M. (2000). Animal and vegetal poles of the mouse egg predict the polarity of the embryonic axis, yet are nonessential for development. Development *127*, 3467–3474.
22. Snell, G.S., and Stevens, L.C. (1966). Early embryology. In Biology of the Laboratory Mouse, E.L. Green, ed. (New York: McGraw-Hill), pp. 205–245.
23. Crossley, P.H., and Martin, G.R. (1995). The mouse Fgf8 gene encodes a family of polypeptides and is expressed in regions that direct outgrowth and patterning in the developing embryo. Development *121*, 439–451.
24. Blum, M., Gaunt, S.J., Cho, K.W., Steinbeisser, H., Blumberg, B., Bittner, D., and De Robertis, E.M. (1992). Gastrulation in the mouse: the role of the homeobox gene goosecoid. Cell *69*, 1097–1106.
25. Lawson, K.A., Meneses, J.J., and Pedersen, R.A. (1991). Clonal analysis of epiblast fate during germ layer formation in the mouse embryo. Development *113*, 891–911.
26. Perea-Gomez, A., Lawson, K.A., Rhinn, M., Zakin, L., Brulet, P., Mazan, S., and Ang, S.L. (2001). Otx2 is required for visceral endoderm movement and for the restriction of posterior signals in the epiblast of the mouse embryo. Development *128*, 753–765.
27. Rivera-Perez, J., Mager, J., and Magnuson, T. (2003). Dynamic morphogenetic events characterize the mouse visceral endoderm. Dev. Biol. *261*, 470–487.
28. Piotrowska, K., and Zernicka-Goetz, M. (2001). Role for sperm in spatial patterning of the early mouse embryo. Nature *409*, 517–521.
29. Gardner, R.L. (2001). Specification of embryonic axes begins before cleavage in normal mouse development. Development *128*, 839–847.
30. Piotrowska, K., Wianny, F., Pedersen, R.A., and Zernicka-Goetz, M. (2001). Blastomeres arising from the first cleavage division have distinguishable fates in normal mouse development. Development *128*, 3739–3748.
31. Fujimori, T., Kurotaki, Y., Miyazaki, J.I., and Nabeshima, Y.I. (2003). Analysis of cell lineage in two- and four-cell mouse embryos. Development *21*, 5113–5122.
32. Hogan. Beddington, R., Costantini, F., and Lacy E. (1994). Manipulating the Mouse Embryo. A Laboratory Manual (Cold Spring Harbor, New York: Cold Spring Harbor Laboratory Press).
33. Wilkinson, D.G. (1990). Whole mount in situ hybridization of vertebrate embryos. In In situ Hybridisation: A Practical Approach, D.G. Wilkinson, ed., (Oxford: IRL Press) pp.75–83.
34. Perea-Gomez, A., Camus, A., Moreau, A., Grieve, K., Moneron, G., Dubois, A., Cibert, C., and Collignon, J. (2004). Initiation of gastrulation in the mouse embryo is preceded by an apparent shift in the orientation of the anterior-posterior axis. Curr. Biol. *14*, this issue, 197–207.